Unimetry: A Phase-Space Reformulation of Special Relativity

Timur Abizgeldin
Independent researcher, Austria
timurabizgeldin@gmail.com

November 2, 2025

Abstract

We propose a compact reformulation of special relativity in which spacetime measures (time and length) are treated as phase velocities, defined as directional derivatives of a single underlying parameter, the flow $\boldsymbol{\chi} \in \mathbb{H}$. In this framework, the observable Minkowski interval emerges as a conserved quantity under a change of parameter from the phase coordinate χ to the observer's proper time τ. Familiar relativistic effects, such as time dilation, the Lorentz factor, the Doppler shift, and relativistic velocity composition, arise as elementary projections and rotations within a Euclidean phase plane. Hyperbolic features of Lorentz kinematics reappear after a reparametrization of time, yielding the classical relations without altering empirical content. We provide closed-form derivations for the longitudinal and transverse Doppler effects, prove a lemma equating the total flow speed to the conserved Minkowski norm, and outline connections to gauge phases, rapidity, and a cosmological time gauge. Composition of non-collinear boosts (quaternionic d-rotations in $\mathbb{H}$) yields a Wigner rotation; in the continuous limit, this gives Thomas precession. Both effects emerge as purely kinematical consequences of the quaternionic phase formalism. The approach is advantageous for applications – especially in modeling non-collinear acceleration of particle beams – where it replaces matrix diagonalizations with algebraic rotor compositions and improves numerical stability.

Keywords: special relativity; phase; rapidity; Doppler shift; Lorentz factor; Wigner rotation; Thomas precession; phase parametrization.

MSC (2020): 83A05; 70A05.

1 Introduction

In classical physics, space and time are taken as absolute and independent entities – a view deeply rooted in Newtonian tradition and characterizing most formulations prior to the early twentieth century. Special relativity revolutionized this perspective by demonstrating that both are intertwined and relative, depending on the observer's state of motion. Yet most conventional treatments still regard spacetime coordinates as fundamental ingredients, with subsequent physical phenomena described in their terms.

This work adopts an alternative viewpoint: instead of starting from space and time as primitives, we treat observed spacetime quantities as derived projections of an underlying phenomenon – a continuous "flow" parameter $\boldsymbol{\chi}$ in quaternionic space $\mathbb{H}$. In this approach, the flow constitutes the primary structure, carrying both local geometric and dynamical information; observable temporal and spatial measures emerge from its decomposition relative to an observer's frame.

This reformulation allows us to re-express relativistic effects – such as time dilation, Lorentz contraction, and the Doppler shift – as geometric consequences of rotations and projections in

Table 1: Derivatives notation used in the paper.

Symbol	Meaning
$\tilde{X}$	χ-parameter derivative with χ having time units; the (dimensionless) phase is $\Phi = \omega\,\chi$.
$\dot{X}$	Proper-time derivative $dX/d\tau$ (lab-time derivatives are written dX/dt explicitly).
X'	Derivative with respect to spatial arclength l or value in a primed inertial frame (as stated locally).

phase space, with quaternion algebra naturally unifying spatial rotations and boosts. The speed of light, in this setting, arises as the constant magnitude of the flow measured locally.

The proposal reorganizes familiar relations in a language aligned with quantum-rotor kinematics, demonstrating the physical equivalence between Lorentz transformations and Euclidean rotations under proper-time parametrization. We realize the phase kinematics with real quaternionic rotors.

Throughout, we use three angles – intrinsic (ζ), gravitational (ϕ), and kinematic (ϑ) – and, when focusing on special relativity (SR), we state the corresponding simplification explicitly. We emphasize that no modification of Einstein's dynamics is proposed; all results are kinematical identities obtained by a change of parameter.

Notation. Tildes, dots, and primes denote derivatives with respect to the time-like parameter, proper time, and spatial arclength:

$$\tilde{X} := \frac{dX}{d\chi}, \qquad \dot{X} := \frac{dX}{d\tau}, \qquad X' := \frac{dX}{dl}.$$

We use c for the speed of light; $\beta := v/c$, $\gamma := 1/\sqrt{1-\beta^2}$, and rapidity defined by $\tanh\eta = \beta$. The subscript l in dx_l denotes spatial components, with $l = 1, 2, 3$ a Cartesian index.

2 Flow concept

2.1 Flow and phase 1-form

Let $\Phi : \mathcal{E} \to \mathbb{R}$ be a scalar dimensionless phase potential on a Euclidean/Hilbert proto-space $(\mathcal{E}, \langle\cdot,\cdot\rangle)$, and the phase 1-form $\alpha := d\Phi$. We use the normalized flow direction $\widehat{\boldsymbol{\chi}} := \nabla\Phi/\|\nabla\Phi\|$ (when $\nabla\Phi \neq 0$), where the gradient is taken with respect to $\langle\cdot,\cdot\rangle$. The physical flow vector is fixed by the calibration in §2.4 as $\boldsymbol{\chi} := c\,\widehat{\boldsymbol{\chi}}$ (so $\|\boldsymbol{\chi}\| \equiv c$ thereafter).

Fix an observer's orthonormal spatial triad $\{\mathbf{e}_1, \mathbf{e}_2, \mathbf{e}_3\} \subset \mathcal{E}$ and let $S = \mathrm{span}\{\mathbf{e}_1, \mathbf{e}_2, \mathbf{e}_3\}$ with orthogonal projectors P_S and $P_{S^\perp}$. Decompose

$$\boldsymbol{\chi} = \boldsymbol{\chi}_S + \boldsymbol{\chi}_\perp, \qquad \boldsymbol{\chi}_S := P_S\boldsymbol{\chi}, \quad \boldsymbol{\chi}_\perp := P_{S^\perp}\boldsymbol{\chi}.$$

Define observable spatial components and the orthogonal magnitude

$$\ell_i := \langle\boldsymbol{\chi}, \mathbf{e}_i\rangle, \qquad \mathbf{l} := \sum_{i=1}^{3} \ell_i\,\mathbf{e}_i, \qquad t_\perp := \|\boldsymbol{\chi}_\perp\| = \sqrt{\|\boldsymbol{\chi}\|^2 - \|\boldsymbol{\chi}_S\|^2},$$

and, when $t_\perp > 0$, the unit direction $\mathbf{e}_t := \boldsymbol{\chi}_\perp/\|\boldsymbol{\chi}_\perp\|$. Here $t_\perp$ always denotes the orthogonal flow magnitude $\|\boldsymbol{\chi}_\perp\|$, while t denotes observer time throughout.

Then the full phase angle Θ and the spatial direction $\mathbf{u}$ used throughout are

$$\cos\Theta = \frac{t_\perp}{\|\boldsymbol{\chi}\|}, \qquad \sin\Theta = \frac{\|\mathbf{l}\|}{\|\boldsymbol{\chi}\|}, \qquad \mathbf{u} = \frac{\mathbf{l}}{\|\mathbf{l}\|} \quad (\|\mathbf{l}\| > 0).$$

Thus the observable space is a 3-manifold embedded in a (minimum) 4-dimensional flow manifold.

Table 2: Notation for § Flow and phase 1-form.

Symbol	Meaning
$\mathcal{E},\ \langle\cdot,\cdot\rangle,\ \|\cdot\|$	Proto-space (Euclidean/Hilbert), its inner product, and the induced norm.
$\Phi : \mathcal{E} \to \mathbb{R}$	Scalar *phase potential*.
$\alpha := d\Phi$	Phase 1-form (exact differential of Φ).
$\widehat{\boldsymbol{\chi}} := \nabla\Phi/\|\nabla\Phi\|$	Normalized flow direction (when $\nabla\Phi \neq 0$). Physical flow: $\boldsymbol{\chi} := c\,\widehat{\boldsymbol{\chi}}$.
$\{\mathbf{e}_1, \mathbf{e}_2, \mathbf{e}_3\}$	Observer's orthonormal spatial triad.
$S = \mathrm{span}\{\mathbf{e}_1, \mathbf{e}_2, \mathbf{e}_3\}$	Observable 3-space; $S^\perp$ is its orthogonal complement.
$P_S,\ P_{S^\perp}$	Orthogonal projectors onto S and $S^\perp$.
$\boldsymbol{\chi}_S := P_S\boldsymbol{\chi},\ \ \boldsymbol{\chi}_\perp := P_{S^\perp}\boldsymbol{\chi}$	Decomposition of the flow into spatial and orthogonal parts ($\boldsymbol{\chi} = \boldsymbol{\chi}_S + \boldsymbol{\chi}_\perp$).
$\ell_i := \langle\boldsymbol{\chi}, \mathbf{e}_i\rangle$	Scalar components of the flow along the triad.
$\mathbf{l} := \sum_{i=1}^3 \ell_i\,\mathbf{e}_i$	Observable spatial projection of the flow ($\mathbf{l} \equiv \boldsymbol{\chi}_S$).
$t_\perp := \|\boldsymbol{\chi}_\perp\| = \sqrt{\|\boldsymbol{\chi}\|^2 - \|\boldsymbol{\chi}_S\|^2}$	Orthogonal ("temporal-fiber") magnitude.
$\mathbf{e}_t := \boldsymbol{\chi}_\perp/\|\boldsymbol{\chi}_\perp\|$	Unit direction along $S^\perp$ (defined when $t_\perp > 0$).
Θ	Full phase angle defined by $\cos\Theta = \dfrac{t_\perp}{\|\boldsymbol{\chi}\|}$ and $\sin\Theta = \dfrac{\|\mathbf{l}\|}{\|\boldsymbol{\chi}\|}$.
$\mathbf{u} := \mathbf{l}/\|\mathbf{l}\|$	Unit spatial direction of the flow (defined when $\|\mathbf{l}\| > 0$).
—	With these definitions, the observable space S is a 3-manifold embedded in a (minimum) 4-dimensional flow manifold $S \oplus \mathrm{span}\{\mathbf{e}_t\}$.

2.2 Flow description

In the flow-based description an object is a collection of elementary "streamlets" (fragments of total object phase flow). Each streamlet admits a co-moving frame in which its spatial projection vanishes and its budget angle equals zero in that frame ("self time" direction).

Larger stable streamlets combinations are Newtonian bodies, which are formed by multiple "self time" flows equally spreaded over the body's 3-surface. Therefore, unlike streamlets bodies have generalized time axis - their time flow isn't already geometric phenomenon.

Postulate. From the ability of bodies to preserve a place within the observable space, we conclude the cyclical nature of streamlets' flows in $\mathcal{E}$:

$$\oint \alpha = 2\pi. \tag{2.1}$$

2.3 Flow of a complex body

Let a (Newtonian) body B be a finite–energy ensemble of streamlets $\mathcal{A} = \{a\}$ with flows $\boldsymbol{\chi}_a$, phase angles Θ_a, and (when defined) unit spatial directions $\mathbf{u}_a \in S$. Assign non-negative weights w_a (fraction of the body's rest energy carried by a) with $\sum_a w_a = 1$, and impose the rest–balance condition

$$\sum_{a\in\mathcal{A}} w_a\,\boldsymbol{\chi}_{S,a} = 0, \qquad \oint \alpha_a = 2\pi \quad \text{(cycle postulate)}. \tag{2.2}$$

Because a body does not possess a single geometric time axis (its streamlets' self–time directions $\mathbf{e}_{t,a}$ are distributed), the effective temporal and spatial responses must be understood

statistically. We therefore introduce the scalar temporal coefficient and the spatial shape tensor (second moment) as

$$T_B := \sum_a w_a \cos^2\Theta_a, \qquad \mathbf{C}_B := \sum_a w_a \sin^2\Theta_a \, \mathbf{u}_a \otimes \mathbf{u}_a, \tag{2.3}$$

where $0 < T_B \leq 1$ and $\mathbf{C}_B$ is a symmetric positive semidefinite tensor on S with $\operatorname{tr}\mathbf{C}_B = \sum_a w_a \sin^2\Theta_a$. Operationally, T_B captures the aggregate fraction of flow carried in the orthogonal (self–time) fiber, while $\mathbf{C}_B$ encodes the anisotropic distribution of spatial projections across the body's 3-surface.

With these ensemble quantities we define the body's *proper time increment* by

$$d\tau_B := \sqrt{T_B}\, d\chi, \tag{2.4}$$

and the body's *self spatial quadratic form* on S by

$$q_B(d\ell) := d\ell^\top \mathbf{C}_B \, d\ell. \tag{2.5}$$

This yields a natural candidate for the body's *self metric* as a quadratic form on $(d\chi, d\ell)$:

$$ds_B^2 \;:=\; c^2\, d\tau_B^2 \;-\; q_B(d\ell) \;=\; c^2 T_B\, d\chi^2 \;-\; d\ell^\top \mathbf{C}_B\, d\ell. \tag{2.6}$$

In the isotropic rest configuration (identical Θ_a and uniform $\mathbf{u}_a$ on S^2) one has $\mathbf{C}_B = \frac{\sin^2\Theta}{3}\mathbf{I}_S$, so (2.6) reduces to the standard Minkowski form up to the overall phase gauge $d\chi$; fixing the gauge by $T_B \equiv 1$ at rest makes $d\tau_B = d\chi$ and restores $q_B(d\ell) = \|d\ell\|^2$. Away from isotropy, $\mathbf{C}_B$ becomes ellipsoidal, and the body's proper metric records the internal orientation texture of its streamlets.

The next section formalizes (2.6), shows how external kinematics (the angle ϑ) and additional phase tilts (intrinsic ζ, gravitational ϕ) renormalize $(T_B, \mathbf{C}_B)$, and derives the usual relativistic effects as deformations of the ensemble moments (2.3).

2.4 Local calibration by the invariant signal speed

The cycle postulate (2.1) fixes the phase scale of each streamlet, but leaves an overall unit choice for the flow magnitude $\|\boldsymbol{\chi}\|$. We now calibrate this scale operationally by the invariant signal speed c.

Calibration postulate (vacuum, isotropic texture). There exist null excitations ("lightlike" streamlets) for which the body-level proper increment vanishes, $d\tau_B = 0$ (equivalently $T_B = 0$), and whose spatial advance per phase increment is direction–independent in vacuum. We define the numerical value of c by the rule

$$\frac{\|d\boldsymbol{\ell}\|}{d\chi} = c \qquad \text{along null flow lines in vacuum.} \tag{2.7}$$

Flow-norm gauge. For any elementary flow, the Euclidean split gives $\|\boldsymbol{\chi}\|^2 = \|\boldsymbol{\chi}_S\|^2 + \|\boldsymbol{\chi}_\perp\|^2$. Along a null flow (orthogonal share vanishes) we have $\|\boldsymbol{\chi}\| = \|\boldsymbol{\chi}_S\| = \|d\boldsymbol{\ell}\|/d\chi$; combining with (2.7) fixes the flow-norm gauge

$$\boxed{\|\boldsymbol{\chi}\| \equiv \mathsf{c}}. \tag{2.8}$$

Consequently, for any decomposition angle Θ introduced in § Flow and phase 1-form,

$$\|\boldsymbol{\chi}_S\| = c\,\sin\Theta, \qquad \|\boldsymbol{\chi}_\perp\| = c\,\cos\Theta. \tag{2.9}$$

Ensemble consequences. For a body B the second moments (2.3) read, after the gauge (2.8),

$$T_B = \sum_a w_a \cos^2\Theta_a, \qquad \operatorname{tr}\mathbf{C}_B = \sum_a w_a \sin^2\Theta_a = 1 - T_B, \tag{2.10}$$

and the intrinsic metric (2.6) becomes

$$\boxed{ds_B^2 = c^2 T_B\, d\chi^2 - d\boldsymbol{\ell}^\top \mathbf{C}_B\, d\boldsymbol{\ell}}. \tag{2.11}$$

Thus c is not introduced dynamically but arises as the *fixed magnitude of the flow* under the calibration (2.7); tilts rotate the budget between the two projections without changing $\|\boldsymbol{\chi}\|$.

Units and phase (resolution of dimensions). We adopt χ as a time-like parameter and define the (dimensionless) phase by $\Phi = \omega\,\chi$, so that $\alpha = d\Phi = \omega\, d\chi$. The cycle postulate $\oint \alpha = 2\pi$ then implies $\oint d\chi = 2\pi/\omega$ along a closed loop. In particular, for null flows in vacuum our calibration $\|d\boldsymbol{\ell}\|/d\chi = c$ fixes the affine advance of χ per emitted cycle via the emission frequency ω.

Invariance under uniform tilts. A uniform phase tilt acts as $\Theta_a \mapsto \Theta_a + \delta$ (see §2.5 below). It preserves the norm (2.8) and merely redistributes the projections as in (2.9). Hence c is invariant, while T_B and $\mathbf{C}_B$ renormalize.

2.5 Intrinsic angle

Using the ensemble second moments (2.3), define

$$C := \sum_a w_a \cos 2\Theta_a, \qquad S := \sum_a w_a \sin 2\Theta_a.$$

There exists a unique $\zeta \in [0, \frac{\pi}{2}]$ such that

$$(\cos 2\zeta,\ \sin 2\zeta) = (C, S) \quad\Longleftrightarrow\quad T_B = \tfrac{1}{2}(1+C) = \cos^2\zeta, \qquad \operatorname{tr}\mathbf{C}_B = \tfrac{1}{2}(1-C) = \sin^2\zeta. \tag{2.12}$$

We call ζ the *effective (intrinsic) angle*: it aggregates the temporal/spatial budget at the level relevant for the intrinsic metric (2.6). In particular,

$$d\tau_B = \cos\zeta\, d\chi, \qquad ds_B^2 = c^2\cos^2\zeta\, d\chi^2 - d\boldsymbol{\ell}^\top \mathbf{C}_B\, d\boldsymbol{\ell},$$

and for an isotropic texture $\mathbf{C}_B = \frac{\sin^2\zeta}{3}\,\mathbf{I}_S$.

Why the double angle. Since ds_B^2 depends only on $\cos^2\Theta_a$ and $\sin^2\Theta_a$, we linearize the ensemble average via $\cos^2\Theta = \frac{1}{2}(1+\cos 2\Theta)$ and $\sin^2\Theta = \frac{1}{2}(1-\cos 2\Theta)$, and collect $(C,S) = \sum_a w_a(\cos 2\Theta_a, \sin 2\Theta_a)$. Then $\zeta = \frac{1}{2}\operatorname{atan2}(S, C)$ ensures $T_B = \cos^2\zeta$ and makes a uniform tilt $\Theta_a \mapsto \Theta_a + \delta$ act additively: $\zeta \mapsto \zeta + \delta$.

Uniform tilt mechanism. A uniform phase tilt by δ transforms

$$C(\delta) = C\cos 2\delta - S\sin 2\delta, \qquad S(\delta) = C\sin 2\delta + S\cos 2\delta,$$

hence

$$\zeta \ \longmapsto\ \zeta' = \zeta + \delta, \qquad T_B(\delta) = \cos^2(\zeta+\delta), \qquad \operatorname{tr}\mathbf{C}_B(\delta) = \sin^2(\zeta+\delta), \tag{2.13}$$

while the full spatial texture remains $\mathbf{C}_B(\delta) = \sum_a w_a \sin^2(\Theta_a+\delta)\,\mathbf{u}_a \otimes \mathbf{u}_a$ (isotropy is preserved by a uniform tilt).

Equations (2.6)–(2.13) complete the object-level construction: the body observes the quadratic geometry ds_B^2, fully controlled by $(\zeta, \mathbf{C}_B)$. Relative measurements between two bodies will be introduced later via their shadows in S.

Remark (symmetric phase pair and nonvanishing spatial share). A frequently used mnemonic for a nonvanishing spatial projection is to pair opposite tilts

$$\boldsymbol{\chi}^{\pm} = R\, e^{\pm\zeta\,\mathbf{l}}, \qquad \boldsymbol{\chi}_l := \frac{\boldsymbol{\chi}^{+} - \boldsymbol{\chi}^{-}}{2} = R\,\mathbf{l}\,\sin\zeta,$$

which matches the decomposition $\boldsymbol{\chi}_0 = \boldsymbol{\chi}_\tau + \boldsymbol{\chi}_l = R\cos\zeta + R\,\mathbf{l}\sin\zeta$. In the ensemble language of (2.3), this construction is not a new dynamics but merely a parametrization of the *second moments*: the spatial budget enters through $\sin^2\Theta_a$ and is fully captured by $\operatorname{tr}\mathbf{C}_B = \sin^2\zeta$ in (2.12). Uniform tilts act additively on the effective angle ζ as in (2.13).

2.6 Three angles

We will use three angles with distinct roles:

- **Intrinsic angle $\boldsymbol{\zeta} \in [0, \frac{\pi}{2}]$**: a second-moment budget angle of the body (no geometric time axis). It is defined by $T_B = \cos^2\zeta$ from (2.12) and governs the intrinsic rate via $d\tau_B = \cos\zeta\, d\chi$. When the same flow characterizes a background medium (not the photon itself), its optical response can be encoded by

  $$v_{\mathrm{ph}}(\text{medium}) = c\,\cos\zeta, \qquad n(\zeta) = \frac{c}{v_{\mathrm{ph}}} = \sec\zeta,$$

  while in the local phase chart ($dt := d\chi$) one has $d\tau_B/dt = \cos\zeta$. *Note:* ζ is a scalar second-moment parameter, not linked to a direction.

- **Gravitational angle $\boldsymbol{\phi}$**: an external tilt field that uniformly rotates streamlet budgets (cf. (2.13)). In the weak, stationary regime it reproduces clock slowing and light delay through an effective index $n_g = \sec\phi$ and $d\tau/dt = \cos\phi$ (no field equations assumed here). Uniform tilts add on second moments, so ζ and ϕ combine as $\zeta \mapsto \zeta + \phi$.

- **Kinematic angle $\boldsymbol{\vartheta}$**: an *observer–relative* directional tilt (introduced in §2.8) built from an observer's split and the unit flow direction. It parameterizes relative motion between bodies; in the SR simplification (below) it becomes the sole angle.

2.7 SR simplification

Whenever along a worldline segment two bodies share the same intrinsic and gravitational tilts (i.e. $\zeta_A = \zeta_B$ and $\phi_A = \phi_B$), one can choose a local comoving chart in which only the directional (kinematic) tilt matters. In SR–focused passages we *set* $\zeta = \phi = 0$ and use $dt := d\chi$; then the kinematic angle ϑ is the only parameter. The standard relations (e.g. the Minkowski interval and the familiar speed/rate identities) will be derived in the next subsection from this setting.

2.8 Minkowski metric derivation

Let A be an observer with orthonormal spatial triad $\{\mathbf{e}_1^A, \mathbf{e}_2^A, \mathbf{e}_3^A\}$, $S^A = \operatorname{span}\{\mathbf{e}_i^A\}$, and time direction $\mathbf{e}_t^A \parallel (S^A)^{\perp}$. For an object with unit flow direction $\widehat{\mathbf{F}} := \boldsymbol{\chi}/\|\boldsymbol{\chi}\|$, define the *observer–object* angle by

$$\widehat{\mathbf{F}} = \cos\vartheta_{|A}\,\mathbf{e}_t^A + \sin\vartheta_{|A}\,\mathbf{u}_{|A}, \qquad \mathbf{u}_{|A} := \frac{P_{S^A}\widehat{\mathbf{F}}}{\|P_{S^A}\widehat{\mathbf{F}}\|} \in S^A.$$

Angle roles (no self time-axis for a composite). For a composite body the intrinsic angle ζ is a second-moment scalar (budget of temporal vs. spatial shares) entering ds_B^2, not a direction. Hence the body has no geometric self time-axis, and there is no notion of "being collinear" with $\mathbf{e}_t^A$. The observer–object angle $\vartheta_{|A}$ is purely directional (built from A's split and $\widehat{\mathbf{F}}$), while ζ controls the intrinsic rate via $T_B = \cos^2\zeta$; they are conceptually independent.

Calibration for the SR sector. To compare with the laboratory rulers in A's frame without invoking any dynamics, we fix a purely kinematic *SR sector*:

1. intrinsic and gravitational tilts are switched off: $\zeta = \phi = 0$ (so $T_B = 1$ in the rest state);
2. the body's spatial texture is isotropic in its rest configuration: $\mathbf{C}_B \propto \mathbf{I}_S$;
3. we take A's lab chart as the phase chart: $dt_A := d\chi$.

With these conventions, the spatial increment seen by A is

$$d\mathbf{x}_{|A} = c\,\sin\vartheta_{|A}\,dt_A\,\mathbf{u}_{|A},$$

and the object's proper time equals the phase chart in this sector: $d\tau_B = d\chi = dt_A$. By $\cos^2 + \sin^2 = 1$ we obtain the Minkowski interval in A's rulers:

$$\boxed{c^2\,d\tau_B^2 \;=\; c^2\,dt_A^2 \;-\; \|d\mathbf{x}_{|A}\|^2} \quad \text{(SR sector: } \zeta = \phi = 0\text{, isotropic rest, } dt_A = d\chi\text{).} \tag{2.14}$$

Remark (outside the SR sector). For general $(\zeta, \mathbf{C}_B)$ the intrinsic interval is always $ds_B^2 = c^2 T_B\,d\chi^2 - d\boldsymbol{\ell}^\top \mathbf{C}_B\,d\boldsymbol{\ell}$. Expressing this in A's lab chart ($dt_A = d\chi$) yields direction-dependent pullbacks via $\mathbf{C}_B$; the standard Minkowski form is recovered precisely when the SR-sector assumptions above hold. The relative ("two-body") kinematics and the emergence of familiar SR effects will be introduced later by comparing the shadows of two objects.

2.9 Symmetry

Two bodies (A and B). Repeating the calibrated SR-sector construction in B's frame gives the same interval form in B's rulers. Swapping "who projects whom" exchanges the splits $(\mathbf{e}_t^A, S^A) \leftrightarrow (\mathbf{e}_t^B, S^B)$ but leaves the Minkowski form invariant.

3 Operations

3.1 Why quaternion algebra

Quaternions form the minimal non-commutative algebra that (i) double-covers $SO(3)$ for rigid 3D rotations; (ii) carries the Hopf fibration $S^3 \to S^2$, separating an internal S^1 time fiber from spatial orientations; and (iii) encodes the non-commutativity responsible for Wigner–Thomas rotations (residual spatial rotations from composing non-collinear boosts) [2, 4, 3].

Simply put one standard sandwich operation in $\mathbb{H}$ of the kind: $\hat{q} \to \hat{r}_1\hat{q}\hat{r}_2$; is sufficient to perform any possible rotation on S^3; the quaternion algebra then simplifies operations on flows relative to the lab triad.

Why a complex slice of a quaternion? For local kinematics any unit direction $\hat{\mathbf{u}}$ singles out the two-dimensional subalgebra $\mathrm{Span}\{1, \hat{\mathbf{u}}\} \cong \mathbb{C} \subset \mathbb{H}$. Working in this complex slice preserves the boost/rotation algebra along $\hat{\mathbf{u}}$ while keeping formulas elementary. When the direction changes, the slice is updated; the full quaternionic structure is retained.

3.2 The spatially linked quaternion

At a point $P \in S$, define

$$q := t_\perp + \mathbf{l} \;=\; t_\perp + l_1\,\mathbf{i} + l_2\,\mathbf{j} + l_3\,\mathbf{k}, \qquad \|q\|^2 = t_\perp^2 + \|\mathbf{l}\|^2 = \|\boldsymbol{\chi}\|^2, \qquad \widehat{q} := \frac{q}{\|q\|}.$$

Hence $\widehat{q} \in S^3 \simeq SU(2)$ encodes the lab-linked state, and a convenient calibration is $\|\boldsymbol{\chi}\| = c$, so that $\|q\| = c$.

Let the observed object internal imaginary basis be $\{I, J, K\} \subset \Im\mathbb{H}$. The observed (lab) orthonormal triad is the conjugated image

$$\mathbf{e_i}(\widehat{q}) = \widehat{q}\,I\,\widehat{q}^{-1}, \qquad \mathbf{e_j}(\widehat{q}) = \widehat{q}\,J\,\widehat{q}^{-1}, \qquad \mathbf{e_k}(\widehat{q}) = \widehat{q}\,K\,\widehat{q}^{-1}.$$

Therefore, it's claimed that the quaternion field over the observable 3D-space manifold defines the direction of the object flow relatively to the lab frame. Considering the time cyclical we introduce the *time fiber* generated by right multiplication with $e^{\frac{\sigma}{2}K}$; its spatial director (shadow) is $\mathbf{n}(\widehat{q}) = \widehat{q}K\widehat{q}^{-1} \in S^2$. This gives a potential link to quantum mechanics spheres.

3.3 Velocity addition

Notation. In unimetry, an inertial boost is a *D-rotation*

$$\mathcal{B}(\hat{\mathbf{u}}, \psi): \quad \mathbf{q} \mapsto d\,\mathbf{q}\,d, \qquad d = \cos\frac{\psi}{2} + \hat{\mathbf{u}}\,\sin\frac{\psi}{2}, \tag{3.1}$$

and a spatial rotation is an *R-rotation*

$$\mathcal{R}(\hat{\mathbf{n}}, \varphi): \quad \mathbf{q} \mapsto r\,\mathbf{q}\,r^{-1}, \qquad r = \cos\frac{\varphi}{2} + \hat{\mathbf{n}}\,\sin\frac{\varphi}{2}. \tag{3.2}$$

Kinematic mapping: $\beta \equiv \mathbf{v}/c = \sin\psi$, $\gamma = 1/\cos\psi$, $\tan\dfrac{\psi}{2} = \dfrac{\gamma\beta}{\gamma+1}$. For quaternionic/GA accounts of rotors and Lorentz boosts see [13, 14, 15].

3.3.1 Wigner rotation

Let d_1, d_2 be D-rotors of two successive boosts. The raw action on any unimetry 4-object is

$$\mathbf{q}' = d_2 d_1\,\mathbf{q}\,d_1 d_2 \equiv L_{12}\,\mathbf{q}\,L_{21}, \qquad L_{12} = d_2 d_1, \quad L_{21} = d_1 d_2. \tag{3.3}$$

Define d_{12} to be the unique D-rotor reproducing the combined spatio–temporal tilt of L_{12}:

$$\boxed{d_{12}\,\mathbf{e}_t\,d_{12} \;=\; L_{12}\,\mathbf{e}_t\,L_{21}, \qquad \Re(d_{12}) \geq 0} \tag{3.4}$$

(the sign choice removes the trivial two-fold ambiguity). Then the Wigner rotor is the residual R-rotation in the symmetric D–R factorization:

$$\boxed{L_{12} = d_{12}\,r_W, \qquad L_{21} = r_W^{-1}\,d_{12}} \tag{3.5}$$

equivalently,

$$\boxed{r_W = \bar{d}_{12}\,L_{12} = L_{21}\,\bar{d}_{12}}. \tag{3.6}$$

Hence the observed map after compensating the tilt is $\bar{d}_{12}\,\mathbf{q}'\,\bar{d}_{12} = r_W\,\mathbf{q}\,r_W^{-1}$.

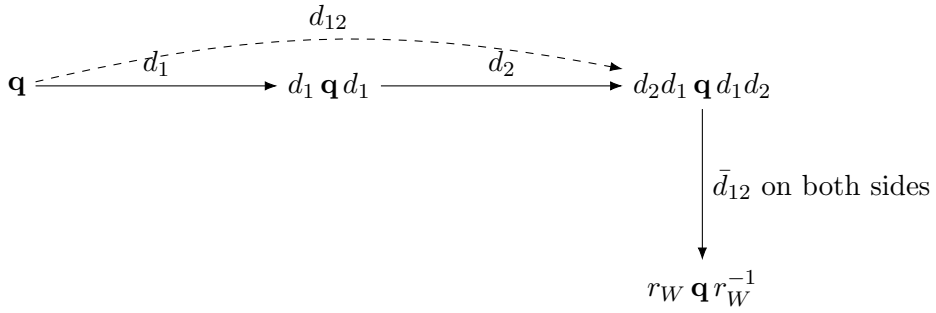

Figure 1: Two successive D-rotations (boosts) and compensation of the net spatio–temporal angle by the conjugate of d_{12}, leaving a pure R-rotation r_W.

3.3.2 Thomas precession

The continuous limit of Wigner rotation for a time-dependent velocity direction $\hat{\mathbf{u}}(t)$ yields

$$\boldsymbol{\omega}_T = (\gamma - 1)\left(\hat{\mathbf{u}} \times \dot{\hat{\mathbf{u}}}\right) = \frac{\gamma^2}{\gamma + 1}\,\frac{\mathbf{a} \times \mathbf{v}}{c^2}, \qquad \gamma = \frac{1}{\cos\psi}. \tag{3.7}$$

For uniform circular motion ($|\mathbf{v}| = \text{const}$) with $\dot{\hat{\mathbf{u}}} = \boldsymbol{\Omega} \times \hat{\mathbf{u}}$ one has $|\boldsymbol{\omega}_T| = (\gamma - 1)\,\Omega$.

3.4 Time fiber, Hopf fibration, and the Bloch/Poincaré spheres.

Consider the map $\pi : S^3 \simeq SU(2) \to S^2$ given by

$$\pi(q) \;=\; \mathbf{n}(q) \;:=\; q\,K\,q^{-1},$$

where $K \in \Im\mathbb{H}$ is a fixed internal unit (the reference "time-axis" in the internal frame). Then:

(i) $U(1)$ fiber by right action. For any $\sigma \in \mathbb{R}$,

$$\mathbf{n}\big(q\,e^{\frac{\sigma}{2}K}\big) = q\,e^{\frac{\sigma}{2}K}\,K\,e^{-\frac{\sigma}{2}K}\,q^{-1} = q\,K\,q^{-1} = \mathbf{n}(q),$$

since K commutes with $e^{\frac{\sigma}{2}K}$. Thus the set

$$\mathcal{F}_{\mathbf{n}} \;=\; \left\{\, q\,e^{\frac{\sigma}{2}K} \;:\; \sigma \in [0, 2\pi)\right\}$$

is the $U(1)$ fiber over the base point $\mathbf{n} \in S^2$. In our kinematics, this right $U(1)$ action is the *time fiber*: internal evolution that preserves the observed spatial director.

(ii) Surjectivity and S^2 base. For any unit $\mathbf{n} \in \Im\mathbb{H}$ there exists $q \in SU(2)$ with $q\,K\,q^{-1} = \mathbf{n}$ (double cover $SU(2) \to SO(3)$). Hence the base of the fibration is the 2-sphere S^2 of spatial directions.

(iii) Link to quantum spheres. Identifying $\Im\mathbb{H} \simeq \mathfrak{su}(2)$ (and, via Pauli matrices, with $\mathbb{R}^3$), the map

$$\mathbf{n}(q) = q\,K\,q^{-1}$$

is the quaternionic form of the Bloch vector for a qubit, or the Stokes vector on the Poincaré sphere for polarization: normalized state rays ($\psi \in \mathbb{C}^2,\ \|\psi\| = 1$) modulo global phase $U(1)$ correspond to points on S^2. Thus $S^3/U(1) \cong S^2$ is the familiar "state-ray" geometry; our time fiber is the same $U(1)$ that is unobservable as a global phase in standard QM, but becomes a *kinematic* degree of freedom here.

(iv) Geometric phase. If $q(\tau)$ traces a loop whose shadow $\mathbf{n}(\tau)$ makes a closed path on S^2, parallel transport in the $U(1)$ fiber accumulates a Berry-type phase $\gamma = \frac{1}{2}\Omega[\mathbf{n}]$, half the solid angle enclosed by the loop on the sphere. In our setting this is an *internal time* holonomy: purely kinematic and arising from the bundle connection induced by the Hopf fibration.

Remark. Left–conjugation $v \mapsto q\, v\, q^{-1}$ rotates lab vectors (changes the *base* point on S^2), whereas right multiplication by $e^{\frac{\sigma}{2}K}$ moves along the *fiber* at fixed $\mathbf{n}$. This cleanly separates spatial reorientation from internal (time/phase) evolution.

4 Phase: operational definition and physical meaning

We will systematically replace hyperbolic functions and nested square roots by the circular trigonometry of a single *phase angle* ϑ, interpreting $\cos\vartheta$ as the temporal projection and $\sin\vartheta$ as the spatial one. This keeps all kinematic identities while avoiding hyperbolic parametrization.

Convention. In this section we track a single body, so $\tau \equiv \tau_B$.

We define the *kinematic angle* $\vartheta \in [0, \frac{\pi}{2})$ of a system with respect to a fixed observer as an **operationally measurable split** of a constant "flow budget" c between temporal and spatial projections:

$$\boxed{\cos\vartheta \equiv \frac{d\tau}{dt}, \qquad \sin\vartheta \equiv \frac{\|\mathbf{v}\|}{c} = \beta, \quad \mathbf{u} = \frac{\mathbf{v}}{\|\mathbf{v}\|}} \tag{4.1}$$

where t is the observer's time, τ is the proper time, and $\mathbf{v}$ is the 3-velocity. The identity $\cos^2\vartheta + \sin^2\vartheta = 1$ then restates the empirical invariance of the Minkowski interval.

Phase state and quaternionic slice. An (inertial) phase state is the pair $(\vartheta, \mathbf{u})$, with $\mathbf{u} \in S^2$. We associate to it the unit quaternion

$$q(\vartheta, \mathbf{u}) = \cos\vartheta + \mathbf{u}\,\sin\vartheta, \qquad \mathbf{u} := u_x\,\mathbf{i} + u_y\,\mathbf{j} + u_z\,\mathbf{k}, \quad \|\mathbf{u}\| = 1, \tag{4.2}$$

that is, a complex slice $\mathbb{C}_{\mathbf{u}} := \mathrm{Span}\{1, \mathbf{u}\} \subset \mathbb{H}$ aligned with $\mathbf{u}$. This is the minimal structure that linearly encodes collinear compositions and naturally induces the Wigner–Thomas rotation for non-collinear boosts via quaternion multiplication.

5 Mapping to standard SR variables

The phase angle ϑ is *not* the rapidity η; they are related by a Gudermann-type [1] bridge

$$\boxed{\beta = \tanh\eta = \sin\vartheta, \qquad \gamma = \cosh\eta = \sec\vartheta, \qquad \tan\frac{\vartheta}{2} = \tanh\frac{\eta}{2}}\,. \tag{5.1}$$

Consequently, all standard kinematic relations follow from circular trigonometry in ϑ:

$$\gamma = \frac{1}{\sqrt{1-\beta^2}} = \sec\vartheta, \qquad k_{\parallel} = e^{\pm\eta} = \frac{1+\tan(\vartheta/2)}{1-\tan(\vartheta/2)}. \tag{5.2}$$

All collinear compositions reduce to angle addition inside the slice $\mathbb{C}_{\mathbf{u}}$.

Collinear composition. For $\mathbf{u}$ fixed,

$$q(\vartheta_2, \mathbf{u})\, q(\vartheta_1, \mathbf{u}) = q(\vartheta_1 \oplus \vartheta_2, \mathbf{u}), \qquad \cos(\vartheta_1 \oplus \vartheta_2) = \cos\vartheta_1\cos\vartheta_2 - \sin\vartheta_1\sin\vartheta_2, \tag{5.3}$$

which implies Einstein's velocity addition

$$\beta_{12} = \sin(\vartheta_1 \oplus \vartheta_2) = \frac{\beta_1 + \beta_2}{1 + \beta_1\beta_2}. \tag{5.4}$$

Non-collinear composition and Wigner–Thomas rotation. For $\mathbf{u}_1 \neq \mathbf{u}_2$ one has the factorization

$$q(\vartheta_2, \mathbf{u}_2)\, q(\vartheta_1, \mathbf{u}_1) = R_W\; q(\vartheta_{12}, \mathbf{u}_{12}), \tag{5.5}$$

where $R_W \in \mathrm{SO}(3)$ is the Wigner–Thomas rotation (a genuine 3D rotation), while $q(\vartheta_{12}, \mathbf{u}_{12})$ is the effective boost in the slice $\mathbb{C}_{\mathbf{u}_{12}}$. The mechanism can be found refined in 3.3.1. The rotation angle and axis can be extracted from the vector part of the quaternion product; a closed expression equivalent to the standard formulas is provided in Appendix A.

6 SR–phase correspondences

Below is a minimal dictionary of correspondences between the hyperbolic SR picture and the circular phase picture.

Quantity	Standard SR (hyperbolic)	Phase picture (circular)
Rapidity	$\eta = \operatorname{artanh}\beta$	$\tanh\eta = \sin\vartheta$
Lorentz factor	$\gamma = \cosh\eta$	$\gamma = \sec\vartheta$
Speed	$\beta = \tanh\eta$	$\beta = \sin\vartheta$
Doppler (longitudinal)	$k = e^{\pm\eta}$	$k = \dfrac{1+\tan(\vartheta/2)}{1-\tan(\vartheta/2)}$
Temporal projection	$\operatorname{sech}\eta$	$\cos\vartheta$

Table 3: One-to-one correspondences between hyperbolic (rapidity) and circular (phase) parametrizations.

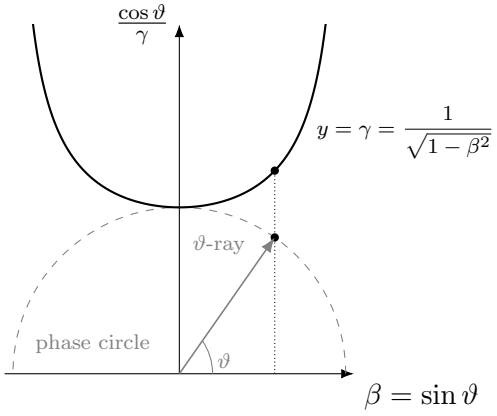

Figure 2: Phase circle vs. Lorentz hyperbola at common $\beta = \sin\vartheta$. Vertical mapping at fixed β illustrates the Gudermann bridge: $\gamma = \sec\vartheta = \cosh\eta$.

7 Phase space

We represent a flow state on a quaternionic *complex slice* $\mathbb{C}_{\mathbf{u}} := \mathrm{Span}\{1, \mathbf{u}\} \subset \mathbb{H}$, where $\mathbf{u} \in S^2$ is the unit spatial direction selected by the observer's split. The unit rotor on this slice is

$$\widehat{q}(\vartheta, \mathbf{u}) := \cos\vartheta + \mathbf{u}\,\sin\vartheta \in S^3 \simeq SU(2),$$

and, under the calibration $\|\boldsymbol{\chi}\| \equiv c$ (cf. §2.4), we parameterize the flow vector as

$$\boldsymbol{\chi}(\vartheta, \mathbf{u}) = c\,\widehat{q}(\vartheta, \mathbf{u}) = c\big(\cos\vartheta + \mathbf{u}\,\sin\vartheta\big). \tag{7.1}$$

Phase-rate projections (observer A). Given an observer A with split $(\mathbf{e}_t^A, S^A)$ and observer–object angle $\vartheta_{|A}$ (see §2.8), the phase-rate components with respect to A are

$$\tilde{X}^0_{|A} := \frac{dx^0_{|A}}{d\chi} = c\cos\vartheta_{|A}, \qquad \tilde{\mathbf{X}}_{|A} := \frac{d\mathbf{x}_{|A}}{d\chi} = c\sin\vartheta_{|A}\,\mathbf{u}_{|A}, \tag{7.2}$$

where $\mathbf{u}_{|A} := P_{S^A}\widehat{\mathbf{F}}/\|P_{S^A}\widehat{\mathbf{F}}\| \in S^A$ is the unit spatial direction as seen by A and $\widehat{\mathbf{F}} := \boldsymbol{\chi}/\|\boldsymbol{\chi}\|$.

These rates satisfy the identity

$$\Big(\frac{ds}{d\chi}\Big)^2 = \big(\tilde{X}^0_{|A}\big)^2 - \big\|\tilde{\mathbf{X}}_{|A}\big\|^2 = c^2\big(1-\sin^2\vartheta_{|A}\big) = c^2\cos^2\vartheta_{|A}. \tag{7.3}$$

which, in the SR simplification ($\zeta = \phi = 0$ and $dt_A := d\chi$), is just the operational split of the fixed budget c into temporal/spatial projections.

Phase-to-observable map (integral form). For any chart x^i adapted to A we have the integral transform

$$x^i(\chi) = x^i(\chi_0) + \int_{\chi_0}^{\chi} \tilde{X}^i_{|A}(u)\,du, \qquad i = 0,1,2,3, \tag{7.4}$$

with $\tilde{X}^0_{|A}$ and $\tilde{\mathbf{X}}_{|A}$ from (7.2). In the SR sector this becomes $t_A(\chi) = t_A(\chi_0) + \int_{\chi_0}^{\chi} du$ and $\mathbf{x}_{|A}(\chi) = \mathbf{x}_{|A}(\chi_0) + \int_{\chi_0}^{\chi} c\sin\vartheta_{|A}(u)\,\mathbf{u}_{|A}(u)\,du$.

Intrinsic vs. directional factors. The intrinsic second-moment angle ζ (§2.5) enters the body's own rate via $d\tau_B/d\chi = \cos\zeta$, while (7.2) is purely directional and built from the observer's split. Outside the SR sector the intrinsic interval is $ds_B^2 = c^2\cos^2\zeta\,d\chi^2 - d\boldsymbol{\ell}^\top\mathbf{C}_B\,d\boldsymbol{\ell}$, and (7.4) remains valid as a kinematic reconstruction of observables from phase rates.

8 Objects: operational catalogue and inference

Scope. This section is a look-up summary. The physics and proofs live in §2.3, §2.5, §2.4, and §9.

Canonical cases

1. **Photon (vacuum).** $T_B = 0,\ d\tau_B = 0,\ \|d\boldsymbol{\ell}\|/d\chi = c$ (Def. (2.7)).
2. **Massive isotropic body.** $\mathbf{C}_B = \frac{\sin^2\zeta}{3}\mathbf{I}$, $d\tau_B = \cos\zeta\,d\chi$, $ds_B^2 = c^2\cos^2\zeta\,d\chi^2 - \frac{\sin^2\zeta}{3}\|d\boldsymbol{\ell}\|^2$.
3. **Anisotropic body.** $\mathbf{C}_B = \sum_{i=1}^3 \lambda_i\,\hat{\mathbf{e}}_i\otimes\hat{\mathbf{e}}_i,\ \lambda_i \ge 0,\ \sum_i\lambda_i = \sin^2\zeta$. Pullbacks along $\hat{\mathbf{e}}_i$ probe λ_i.
4. **Effective medium (ζ only).** $d\tau/dt = \cos\zeta,\ n(\zeta) = \sec\zeta$ (cf. §10).

Parameter inference

- *Rate split at rest.* With $\vartheta = 0,\ \phi = 0$: $\cos\zeta = \big(d\tau_B/dt\big)_{\text{meas}}$.
- *Directional pullbacks.* Measure ds_B^2 for small $d\boldsymbol{\ell}$ along several lab directions; fit the quadratic form $q_B = d\boldsymbol{\ell}^\top\mathbf{C}_B\,d\boldsymbol{\ell} \Rightarrow$ eigenpairs $(\lambda_i, \hat{\mathbf{e}}_i)$.
- *Factorization with gravity/kinematics.* Use $d\tau/dt = \cos\zeta\cos\phi\cos\vartheta$ to separate ϕ (clock angle) from ζ via e.g. static vs moving protocols (see §10).

Ensemble composition

For streamlets a with weights w_a: $T_B = \sum_a w_a \cos^2\Theta_a$, $\mathbf{C}_B = \sum_a w_a \sin^2\Theta_a\, \mathbf{u}_a \otimes \mathbf{u}_a$ (Eq. (2.3)).

Non-collinear boosts

Composition induces a spatial Wigner rotation on orientations without altering the scalar rate factorization; see §3.3.1, §3.3.2.

9 Phase-derivative view

Scope. This section repackages core identities in the language of *phase derivatives*, using only notions already introduced (§2.4–2.8). No new kinematics is postulated.

Notation recap (from §7). Phase–rate components for an observer A are

$$\tilde{X}^0_{|A} = \frac{dx^0_{|A}}{d\chi} = c\,\cos\vartheta_{|A}, \qquad \tilde{\mathbf{X}}_{|A} = \frac{d\mathbf{x}_{|A}}{d\chi} = c\,\sin\vartheta_{|A}\,\mathbf{u}_{|A}, \tag{7.2}$$

and obey the identity

$$\Big(\frac{ds}{d\chi}\Big)^2 = \big(\tilde{X}^0_{|A}\big)^2 - \big\|\tilde{\mathbf{X}}_{|A}\big\|^2 = c^2\big(1-\sin^2\vartheta_{|A}\big) = c^2\cos^2\vartheta_{|A}. \tag{7.3}$$

A change of parameter $\chi \mapsto \tau$ acts by the Jacobian $\mathcal{J} := \dfrac{d\chi}{d\tau}$:

$$\dot{X}^i = \frac{dx^i}{d\tau} = \mathcal{J}\,\tilde{X}^i, \qquad \dot{X} \equiv d/d\tau, \quad \tilde{X} \equiv d/d\chi. \tag{9.1}$$

9.1 Minkowski–phase equality of invariants

Theorem. For any worldline segment and any observer A,

$$\boxed{\tilde{H} \;=\; \dot{S}}, \qquad \tilde{H}^2 := \big(\tilde{X}^0_{|A}\big)^2 + \big\|\tilde{\mathbf{X}}_{|A}\big\|^2, \quad \dot{S}^2 := \big(\dot{X}^0_{|A}\big)^2 - \big\|\dot{\mathbf{X}}_{|A}\big\|^2. \tag{9.2}$$

Proof. By (9.1), $\dot{X}^i = \mathcal{J}\,\tilde{X}^i$, hence

$$\dot{S}^2 = (\mathcal{J}\tilde{X}^0)^2 - \|\mathcal{J}\tilde{\mathbf{X}}\|^2 = \mathcal{J}^2\Big(\tilde{X}^{02} - \|\tilde{\mathbf{X}}\|^2\Big) = \mathcal{J}^2\Big(\frac{ds}{d\chi}\Big)^2 = \Big(\frac{ds}{d\tau}\Big)^2.$$

At the same time, $\tilde{H}^2 = \tilde{X}^{02} + \|\tilde{\mathbf{X}}\|^2 = c^2$ in the SR gauge (§2.7), and $ds/d\tau = c$ by the operational split $\cos\vartheta = d\tau/dt$, $\sin\vartheta = \|\mathbf{v}\|/c$ (§4). Therefore $\tilde{H} = \dot{S} = c$. □

Reading. In words: the Euclidean norm of the phase–rate vector equals the Minkowski norm of the observable rate vector. The equality (9.2) is the derivative form of "the same budget seen in two parametrizations".

9.2 Photon time: null interval and phase parameter

For a lightlike flow in vacuum, the body's intrinsic quadratic form gives $ds_B^2 = 0$ (§2.4), hence the body-level proper increment vanishes:

$$\boxed{d\tau_B = 0 \quad \text{(null flow, vacuum)}}. \tag{9.3}$$

Nevertheless the phase parameter χ advances and serves as an *affine* parameter along the ray. With the calibration (2.7) we have

$$\frac{\|d\boldsymbol{\ell}\|}{d\chi} = \mathsf{c}, \qquad \Rightarrow \quad \chi = \text{(cycle counter)}. \tag{9.4}$$

Under the convention $\Phi = \omega\,\chi$, one cycle corresponds to $\Delta\chi = 2\pi/\omega$, so χ counts wavefronts affinely while the intrinsic metric remains null ($d\tau_B = 0$).

At unit frequency, $\nu := d\chi/d\tau = 1$, the phase equals the proper-time parameter used as an affine label of wavefronts; no contradiction with (9.3) arises because τ here is a *chosen* parameter for counting cycles, while the intrinsic metric length remains null.

9.3 Relativistic Doppler as a phase–kinematic theorem

We derive the Doppler law purely from the phase split, without hyperbolic parametrization or dynamics.

Setup. Define frequency as the phase growth rate in proper time, $\nu := d\chi/d\tau$, and consider two successive wavefronts separated by the same phase increment $\Delta\chi$ for the source and the observer. Then

$$\frac{\nu_{\text{obs}}}{\nu_{\text{src}}} = \frac{d\chi/d\tau_{\text{obs}}}{d\chi/d\tau_{\text{src}}} = \frac{d\tau_{\text{src}}}{d\tau_{\text{obs}}}. \tag{9.5}$$

In the SR sector ($\zeta = \phi = 0$) the observer at rest has $d\tau_{\text{obs}} = dt_{\text{obs}}$, and for the (possibly moving) source $dt_{\text{src}} = \gamma\, d\tau_{\text{src}}$ with $\gamma = \sec\vartheta$, $\beta = \sin\vartheta$.

Longitudinal case. During the emission interval $dt_{\text{src}} = \gamma\, d\tau_{\text{src}}$ (measured in the observer's lab chart) the source shifts by $\pm\beta c\, dt_{\text{src}}$ along the line of sight ("+" receding, "−" approaching). The reception interval is the emission interval plus the change in light flight time:

$$dt_{\text{obs}} = dt_{\text{src}}\,\big(1 \pm \beta\big) = \gamma\, d\tau_{\text{src}}\,\big(1 \pm \beta\big).$$

With (9.5) and $d\tau_{\text{obs}} = dt_{\text{obs}}$ this gives the Doppler factor

$$\boxed{\frac{\nu_{\text{obs}}}{\nu_{\text{src}}} = \frac{1}{\gamma(1 \pm \beta)}} = \sqrt{\frac{1 \mp \beta}{1 \pm \beta}} = \sec\vartheta\,(1 \mp \sin\vartheta) = e^{\mp\eta}, \tag{9.6}$$

where the equivalent forms use $\beta = \sin\vartheta$, $\gamma = \sec\vartheta$, and the Gudermann bridge (5.1).

Transverse case. For $\varphi = 90^\circ$ (emission orthogonal to the relative velocity in the observer's frame), the geometric flight-time correction vanishes, hence

$$\boxed{\frac{\nu_{\text{obs}}}{\nu_{\text{src}}} = \frac{1}{\gamma} = \cos\vartheta}. \tag{9.7}$$

General line-of-sight angle. Let φ be the angle between the source velocity and the line of sight in the observer's frame. Only the LOS component $\beta\cos\varphi$ changes the flight time; repeating the above,

$$\boxed{\frac{\nu_{\rm obs}}{\nu_{\rm src}} = \frac{1}{\gamma\,(1-\beta\cos\varphi)} \;=\; \gamma\,(1-\beta\cos\varphi)^{-1}}\,. \tag{9.8}$$

Equivalently, in phase variables, $\nu_{\rm obs}/\nu_{\rm src} = \sec\vartheta\,\big(1-\sin\vartheta\cos\varphi\big)^{-1}$.

Corollary (with intrinsic/gravitational tilts). Outside the pure SR sector, the total redshift factorizes:

$$1+z_{\rm tot} = \frac{\nu_{\rm src}}{\nu_{\rm obs}} = \underbrace{\gamma(1-\beta\cos\varphi)}_{\text{kinematic}} \times \underbrace{\frac{\cos\zeta_{\rm obs}\cos\phi_{\rm obs}}{\cos\zeta_{\rm src}\cos\phi_{\rm src}}}_{\text{intrinsic \& gravitational}}\,,$$

which reproduces (11.3) upon identifying the kinematic part with (9.8).

Infinitesimal form (longitudinal). Taking the differential of $\ln(\nu_{\rm obs}/\nu_{\rm src})$,

$$\boxed{d\ln\frac{\nu_{\rm obs}}{\nu_{\rm src}} = \mp\,d\eta = \mp\,\sec\vartheta\,d\vartheta = \mp\,\gamma^2\,d\beta}\,, \tag{9.9}$$

with the upper sign for receding ("+" in (**??**)) and lower for approaching. Equation (9.9) is the *phase–derivative* Doppler law.

Transverse case. For $\varphi = 90^\circ$ in the observer's frame the flight-time correction vanishes, so $\nu_{\rm obs}/\nu_{\rm src} = 1/\gamma$ and

$$d\ln\frac{\nu_{\rm obs}}{\nu_{\rm src}} = -\,d\ln\gamma = -\beta\gamma^2\,d\beta. \tag{9.10}$$

General LOS angle (fixed geometry). If φ is the angle between the velocity and the line of sight in the observer's frame and $d\varphi = 0$, then from $\nu_{\rm obs}/\nu_{\rm src} = 1/\big[\gamma(1-\beta\cos\varphi)\big]$ one gets

$$d\ln\frac{\nu_{\rm obs}}{\nu_{\rm src}} = -\Big[\beta\gamma^2 - \frac{\cos\varphi}{1-\beta\cos\varphi}\Big]\,d\beta \;=\; -\,d\eta \;\;\text{when}\;\; \varphi = 0,\pi. \tag{9.11}$$

Together, (9.2), (9.3)–(9.4), and (9.9)–(9.11) show how *phase derivatives* encode: (i) equality of observable and phase invariants; (ii) the null nature of photon proper time with χ as an affine counter; (iii) the Doppler law, both finite and in instantaneous differential form.

10 Unified temporal effects in phase space

We factor all time-related effects through a single phase tilt structure. Let the intrinsic (ζ), gravitational (ϕ), and kinematic (ϑ) angles be independent contributors to the phase tilt at a point. Define the local *time-rate factor*

$$\frac{d\tau}{dt} \;=\; \cos\zeta\;\cos\phi\;\cos\vartheta, \qquad n_{\rm tot} \;:=\; \sec\zeta\;\sec\phi\;\sec\vartheta, \tag{10.1}$$

where $n_{\rm tot}$ plays the role of an effective (phase) refractive index for light propagation. Accordingly, the coordinate light-travel time along a spatial curve Γ is

$$t_\Gamma \;=\; \frac{1}{c}\int_\Gamma n_{\rm tot}\,ds. \tag{10.2}$$

Lemma (Unified time-rate). In the unimetry phase representation, the proper-to-lab time rate and the optical length factorize as in (10.1)–(10.2). Setting any subset of angles to zero recovers the corresponding standard effects:

- **Special relativity (vacuum SR):** $\zeta = 0,\ \phi = 0 \Rightarrow d\tau/dt = \cos\vartheta = 1/\gamma$ (kinematic time dilation).
- **Gravitational clocks (static weak field):** $\zeta = 0,\ \vartheta = 0 \Rightarrow d\tau/dt = \cos\phi$ (gravitational redshift/clock rate); calibration of ϕ reproduces the usual $\sqrt{g_{00}}$.
- **Shapiro delay (gravitational contribution to TOF):** with $\zeta = 0,\ \vartheta = 0$, (10.2) yields $t_\Gamma = (1/c)\int \sec\phi\, ds$; the excess over $\int ds/c$ is the Shapiro time delay.
- **Intrinsic/evolutionary tilt:** $\phi = 0,\ \vartheta = 0 \Rightarrow d\tau/dt = \cos\zeta,\ n_{\rm tot} = \sec\zeta$ (useful as a time gauge in cosmological/effective-medium contexts).

Remarks. (i) The factorization in (10.1) is the phase-space counterpart of composing independent tilts; it preserves the conserved Minkowski norm once time is reparameterized by τ. (ii) For vacuum SR we simply set $\zeta = 0$ and work with ϑ; for pure gravitational timing we set $\vartheta = 0$ and use ϕ. (iii) Non-collinear boost composition acts on ϑ via quaternionic rotors and induces a Wigner/Thomas residual *spatial* rotation without altering (10.1).

11 Gravity as a phase rotation: local tetrads and clock angle

On a curved background $(\mathcal{M}, g)$ we work with orthonormal tetrads $e_a{}^\mu$ such that $g_{\mu\nu}e_a{}^\mu e_b{}^\nu = \eta_{ab}$ and take the observer's time leg to be $e_0{}^\mu$. We apply the gravitational (clock) angle ϕ as

$$\cos\phi \;:=\; e^0{}_\mu\, u^\mu \;=\; \frac{d\tau_{\rm stat}}{dt} \;=\; \sqrt{-g_{00}} \qquad \text{(stationary case)}. \tag{11.1}$$

Kinematics remains encoded by the phase angle ϑ in the slice $\mathbb{C}_{\mathbf{u}}$, with $\cos\vartheta = d\tau/d\tau_{\rm stat}$. Therefore the proper time factorizes as

$$d\tau \;=\; dt\,\cos\phi\,\cos\vartheta, \qquad d\mathbf{x} \;=\; c\,dt\,\sin\vartheta\,\mathbf{u}, \tag{11.2}$$

and the total redshift factorizes into kinematic and gravitational parts:

$$1 + z_{\rm tot} \;=\; \frac{\cos\vartheta_{\rm em}}{\cos\vartheta_{\rm obs}} \;\times\; \frac{\cos\phi(x_{\rm em})}{\cos\phi(x_{\rm obs})}. \tag{11.3}$$

For static emitter/observer ($\vartheta_{\rm em} = \vartheta_{\rm obs} = 0$) one recovers the standard gravitational redshift $1 + z_g = \sqrt{\frac{-g_{00}(x_{\rm obs})}{-g_{00}(x_{\rm em})}}$. In the weak-field limit $g_{00} \simeq -(1 + 2\Phi/c^2)$ this gives $z_g \simeq (\Phi_{\rm obs} - \Phi_{\rm em})/c^2$.

Beyond static fields. In a 3+1 split $ds^2 = -N^2c^2dt^2 + h_{ij}(dx^i + N^i dt)(dx^j + N^j dt)$ one may identify $\cos\phi := N$ in the observer's tetrad, which keeps (11.2)–(11.3) coordinate-agnostic. Uniform acceleration (Rindler) accumulates phase according to $d\vartheta = \kappa\, dt$ inside the local slice, consistently reproducing accelerated-frame kinematics when combined with the clock angle ϕ.

Outlook

The unimetry framework developed here provides a versatile foundation for future theoretical developments in both relativity and quantum physics. The following directions emerge as particularly promising:

- **Extension to General Relativity.** The modular phase decomposition is well suited for the introduction of curved metrics, potentially allowing gravitational redshift, time delay (Shapiro effect), and even curvature-driven precessions to be recast in the language of phase tilts and generalized rotors. Realizing Einstein's dynamics for gravitational fields in this formalism is a natural next step, especially via the local tetrad and clock angle structures already sketched.

- **Quantum Connections.** Given the central role of phase, rotors, and symmetry groups (notably the demonstration of Hopf fibration structure), the unimetry formalism can serve as a stepping stone toward a deeper unification between relativistic and quantum frameworks, possibly via geometric quantization or generalized qubit/Bloch-sphere analogues.

- **Physical and Experimental Applications.** The structure is already suited for reinterpretation and numerical simulation of phenomena involving non-collinear accelerations, such as in advanced particle beam physics or optical systems with phase media. This computational potential deserves further methodological and comparative exploration.

- **Generalizations and Group Theory.** The embedding of Lorentzian kinematics within a more general Euclidean group-theoretic framework (potentially encompassing de Sitter or conformal transformations) may suggest further extensions, including nontrivial topologies, higher dimensions, or self-dual (instanton-like) solutions.

In summary, by replacing the traditional spacetime paradigm with a geometric flow in phase space, unimetry opens avenues for new mathematical structures and connections among relativity, geometry, and quantum theory. Its broader success will depend on future progress in developing the gravitational and quantum sectors and on the demonstration of concrete computational and experimental advantages.

References

[1] NIST Digital Library of Mathematical Functions, §4.23 "Gudermannian Function", `https://dlmf.nist.gov/4.23`.

[2] H. Hopf, "Über die Abbildungen der dreidimensionalen Sphäre auf die Kugelfläche," *Mathematische Annalen* **104** (1931) 637–665. doi:10.1007/BF01457962.

[3] L. H. Thomas, "The Motion of the Spinning Electron," *Nature* **117** (1926) 514. doi:10.1038/117514a0.

[4] E. P. Wigner, "On Unitary Representations of the Inhomogeneous Lorentz Group," *Annals of Mathematics* **40** (1939) 149–204. doi:10.2307/1968551.

[5] M. V. Berry, "Quantal phase factors accompanying adiabatic changes," *Proceedings of the Royal Society A* **392** (1984) 45–57. doi:10.1098/rspa.1984.0023.

[6] I. I. Shapiro, "Fourth Test of General Relativity," *Phys. Rev. Lett.* **13** (1964) 789–791. doi:10.1103/PhysRevLett.13.789.

[7] W. Rindler, *Relativity: Special, General, and Cosmological*, 2nd ed., Oxford University Press, 2006.

[8] C. W. Misner, K. S. Thorne, J. A. Wheeler, *Gravitation*, W. H. Freeman, 1973.

[9] J. D. Jackson, *Classical Electrodynamics*, 3rd ed., Wiley, 1999.

[10] A. Einstein. Zur Elektrodynamik bewegter Körper. *Annalen der Physik*, 17:891–921, 1905. (English translation: On the electrodynamics of moving bodies.)

[11] W. Rindler. *Relativity: Special, General, and Cosmological.* Oxford University Press, 2nd ed., 2006.

[12] E. F. Taylor and J. A. Wheeler. *Spacetime Physics.* W. H. Freeman, 2nd ed., 1992.

[13] W. R. Hamilton, *On quaternions; or on a new system of imaginaries in algebra*, Philosophical Magazine **25**, 10–13 (1844).

[14] D. Hestenes and G. Sobczyk, *Clifford Algebra to Geometric Calculus*, Reidel, 1984.

[15] C. Doran and A. Lasenby, *Geometric Algebra for Physicists*, Cambridge University Press, 2003.

A Equivalence to the classical Wigner rotation

We sketch an intrinsic quaternionic proof that the unimetry expression for the Wigner rotation coincides with the standard special-relativistic formula.

Step 1: product of two D-rotors. For $d_i = \cos\frac{\psi_i}{2} + \hat{\mathbf{u}}_i \sin\frac{\psi_i}{2}$,

$$d_2 d_1 = (c_2 c_1 - s_2 s_1 \cos\theta) + \Big(c_2 s_1 \hat{\mathbf{u}}_1 + s_2 c_1 \hat{\mathbf{u}}_2 + s_2 s_1\, \hat{\mathbf{u}}_2 \times \hat{\mathbf{u}}_1\Big), \tag{A.1}$$

with $c_i = \cos(\psi_i/2)$, $s_i = \sin(\psi_i/2)$ and $\cos\theta = \hat{\mathbf{u}}_2 \cdot \hat{\mathbf{u}}_1$.

Step 2: symmetric D–R factorization. Define d_{12} by $d_{12}\,\mathbf{e}_t\,d_{12} = L_{12}\,\mathbf{e}_t\,L_{21}$ and set $r_W = \bar{d}_{12}\,L_{12} = L_{21}\,\bar{d}_{12}$. Then r_W fixes $\mathbf{e}_t$ and is a pure spatial rotor, so $r_W = \cos\frac{\phi}{2} + \hat{\mathbf{n}}\sin\frac{\phi}{2}$ with $\hat{\mathbf{n}} \parallel \hat{\mathbf{u}}_2 \times \hat{\mathbf{u}}_1$. Matching scalar and bivector parts gives

$$\tan\frac{\phi}{2} = \frac{s_1 s_2\, \sin\theta}{c_1 c_2 + s_1 s_2\, \cos\theta}. \tag{A.2}$$

Step 3: map to rapidities. With the substitutions $\sin(\psi/2) \mapsto \sinh(\eta/2)$, $\cos(\psi/2) \mapsto \cosh(\eta/2)$, $\tan(\psi/2) \mapsto \tanh(\eta/2)$ (where $\tanh\eta = \beta$, $\cosh\eta = \gamma$), (A.2) becomes the textbook Wigner angle:

$$\tan\frac{\phi}{2} = \frac{\sinh\frac{\eta_1}{2}\,\sinh\frac{\eta_2}{2}\,\sin\theta}{\cosh\frac{\eta_1}{2}\,\cosh\frac{\eta_2}{2} + \sinh\frac{\eta_1}{2}\,\sinh\frac{\eta_2}{2}\,\cos\theta}, \tag{A.3}$$

with axis along $\hat{\mathbf{u}}_2 \times \hat{\mathbf{u}}_1$. This circular–hyperbolic correspondence is classical; cf. Gudermann [1].

B A worked example — Wigner angle in hyperbolic vs phase parametrizations with a stability note

Closed-form formulae. Let $\boldsymbol{\beta}_i$ $(i = 1, 2)$ be two non-collinear boost velocities with magnitudes $\beta_i = \|\boldsymbol{\beta}_i\| < 1$ and let χ be the angle between their *directions*. The Thomas–Wigner rotation R_W generated by the composition of boosts has axis $\hat{\mathbf{n}} \parallel \hat{\boldsymbol{\beta}}_2 \times \hat{\boldsymbol{\beta}}_1$ and angle ψ_W given by either of the following equivalent half–angle forms:

$$\tan\frac{\psi_W}{2} = \frac{\sin\chi\,\tanh\frac{\eta_1}{2}\,\tanh\frac{\eta_2}{2}}{1 + \cos\chi\,\tanh\frac{\eta_1}{2}\,\tanh\frac{\eta_2}{2}}, \qquad \beta_i = \tanh\eta_i, \tag{B.1}$$

$$\tan\frac{\psi_W}{2} = \frac{\sin\chi\,\tan\frac{\vartheta_1}{2}\,\tan\frac{\vartheta_2}{2}}{1 + \cos\chi\,\tan\frac{\vartheta_1}{2}\,\tan\frac{\vartheta_2}{2}}, \qquad \beta_i = \sin\vartheta_i. \tag{B.2}$$

Numerically stable and parametrization–agnostic is the identity

$$\tanh\frac{\eta_i}{2} = \tan\frac{\vartheta_i}{2} = \frac{\gamma_i\beta_i}{1+\gamma_i} = \frac{\beta_i}{1+\sqrt{1-\beta_i^2}} =: t_i, \qquad \gamma_i = (1-\beta_i^2)^{-1/2}. \tag{B.3}$$

With t_i from (B.3), both (B.1)–(B.2) reduce to

$$\psi_W = 2\,\mathrm{atan2}\Big(\sin\chi\, t_1 t_2,\ 1+\cos\chi\, t_1 t_2\Big), \tag{B.4}$$

which avoids overflow/underflow and ensures the correct quadrant.

Example A (orthogonal boosts, moderate γ). Take $\boldsymbol{\beta}_1 = (0.8, 0, 0)$ and $\boldsymbol{\beta}_2 = (0, 0.6, 0)$, so $\chi = \pi/2$. From (B.3) one finds $t_1 = \frac{1}{2}$ and $t_2 = \frac{1}{3}$ exactly, hence $\tan(\psi_W/2) = t_1 t_2 = \frac{1}{6}$ and

$$\boxed{\psi_W = 2\arctan\frac{1}{6} = 0.3302973548292537 \text{ rad} = 18.924644416051237^\circ}$$

Both parametrizations (B.1) and (B.2) coincide to machine precision. A direct 4×4 Lorentz–matrix composition followed by polar decomposition of the spatial block recovers $\psi_W = 0.3302973548292533$ rad (agreement to $< 5\times10^{-16}$ rad).

Example B (ultra–relativistic, small inter–direction angle). Let $\boldsymbol{\beta}_1 = (0.999999, 0, 0)$ and $\boldsymbol{\beta}_2 = 0.9999(\cos 1^\circ, \sin 1^\circ, 0)$ so that $\chi = 1^\circ$. Then (B.3) gives $t_1 = 0.9985867853779378$, $t_2 = 0.9859568136154433$ and

$$\boxed{\psi_W = 2\,\mathrm{atan2}\big(\sin 1^\circ\, t_1 t_2,\ 1+\cos 1^\circ\, t_1 t_2\big) = 0.0173175319077011 \text{ rad} = 0.9922214898944112^\circ}$$

The same value is obtained from either (B.1) or (B.2). A double–precision Lorentz–matrix calculation with orthonormalization of the spatial block yields $\psi_W = 0.0173175044768120$ rad (agreement to $\sim 3\times10^{-8}$ rad; the residual is purely numerical).

Stability and accumulated error (practical note).

- **Half–angle is key.** Computing via (B.3) and (B.4) is markedly more stable than naively evaluating $\eta_i = \operatorname{artanh}\beta_i$ followed by $\sinh(\eta_i/2), \cosh(\eta_i/2)$, especially for $\gamma \gtrsim 10^2$ or tiny χ where subtractive cancellation appears in the denominator of (B.1).
- **Single vs double precision.** For Example A, all routes (phase/hyperbolic/matrix) agree within $\sim 10^{-7}$ rad even in single precision. For Example B, the analytic half–angle formula (B.4) remains well-behaved in single precision ($\psi_W = 0.01731725$ rad; deviation $\sim 3\times10^{-7}$ rad), while a direct 4×4 matrix composition in single precision becomes ill–conditioned (eigen–based orthonormalization fails to converge), a manifestation of catastrophic rounding at $\gamma \sim 10^3$.
- **Error accumulation under repetitions.** If the same pair of boosts is applied repeatedly, the rotation axis $\hat{\mathbf{n}}$ is fixed and the angle adds linearly mod 2π. In finite precision, composing dense Lorentz matrices N times amplifies roundoff roughly linearly in N, whereas evaluating (B.4) per step and accumulating the angle avoids the growth of matrix–multiplication conditioning.

Recommendation (for reproducible numerics). Use (B.3) to form t_i directly from β_i, then evaluate (B.4) with `atan2`. When a matrix route is unavoidable, extract the spatial rotation by removing the net boost and projecting the 3×3 block to SO(3) via a polar decomposition before reading off ψ_W.